ISSN 2176-5480

22nd International Congress of Mechanical Engineering (COBEM 2013)
November 3-7, 2013, Ribeirão Preto, SP, Brazil

MODEL IDENTIFICATION TECHNIQUE AND PID CONTROLLER FOR A STEWART PLATFORM

Ricardo Breganon
Instituto Federal do Paraná, Av. Dr. Tito, s/n, Jardim Panorama, Jacarezinho – PR.
ricardo.breganon@ifpr.edu.br

Mateus Moreira de Souza
Fabio Toledo Bonemer De Salvi
Eduardo Morgado Belo
Escola de Engenharia de São Carlos, Universidade de São Paulo, Av. Trabalhador São Carlense, 400, Pq Arnold Schmidt, São Carlos – SP.
mateusmoreiradesouza@yahoo.com.br; fabiodesalvi@yahoo.com.br; belo@sc.usp.br.

Rodrigo Cristian Lemes
Instituto Federal de São Paulo, Rodovia Washington Luís, km 235, São Carlos – SP.
professorlemes@yahoo.com

Abstract. *In the last years there has been great interest in studying parallel manipulators, applied mostly in flight simulators, with six degrees of freedom. The interest in parallel kinematic structures is motivated by its high stiffness and excellent positioning capability compared to serial kinematic structures. Moreover, as the electromechanical actuators are positioned on a base, they do not need support or unit mass of other actuators, dealing with weighty loads and still be energy efficient, considering that several actuators act on the same body. This paper presents the dynamic modeling of a motion platform with six degrees of freedom for studies on flight simulators and the development of a PID controller (Proportional, Integrative and Derivative). The model of the actuators was obtained using step input voltage in the engines and measuring its displacement through encoders and calibration curves. The control system consists of PID controllers, whose gains are adjusted based on the model of the actuator in order to control the position and orientation of the flight simulator. The actuating signal is obtained utilizing the error signals generated by comparing the desired trajectory of the manipulator and the length of the actuators. The system identification and control were used in the Stewart platform designed in the Airspace Control Laboratory of the Engineering School of São Carlos of the University of São Paulo, showing the efficiency of the applied technique.*

Keywords: *Stewart Platform, PID Controller, System Identification, Orientation Controller, Position Controller.*

1. INTRODUCTION

Parallel structures have emerged in the 60s associated with flight simulators and, from the late '80s, parallel manipulators with rigid actuators have been used as the basis for simulations with various degrees of freedom. Stewart (1965) proposed a parallel structure with six degrees of freedom drawn from the adaptation of a flight simulator to a structure known since 1947 as Gough platform used to build a machine to test tires. This structure became known as Stewart Platform (Dasgupta e Mruthyunjaya, 2000).

Currently various systems configurations and mechanisms for motion control with multiple degrees of freedom are being studied standing out closed kinematic parallel manipulators called Stewart Platform (Becerra-Vargas, 2009). This paper presents the modeling and implementation of a PID controller design for a Stewart platform control developed in the Airspace Control Laboratory of the Engineering School of São Carlos of the University of São Paulo, shown in Fig.1.

For position control, the kinematics of a manipulator is an important aspect to be considered, where from the direct kinematics, the position and orientation of the end effectors is determined on the basis of joint variables. The inverse kinematic model is required for the calculation of the displacements of the joints when the movements are considered in the workspace, such as the movement of the end effectors along a trajectory (Moretti, 2010).

ISSN 2176-5480

Figure 1: Stewart Platform.

2. INVERSE KINEMATICS

In the design of a control system for position and attitude of the movable platform of a Stewart platform is necessary to know the inverse kinematics of this mechanism. The inverse kinematics uses the position and attitude of the movable platform with respect to the fixed platform to obtain the lengths of the actuators and can be addressed using tensor modeling (Zipfel, 2000) or modeling based on linear algebra (Nguyen et al., 1993). The modeling using linear algebra is presented in this paper.

The positions of the joints connecting the platforms with the actuators are defined in two coordinate systems. A system with origin in the center of the fixed platform *F* and axis *xf* pointing between joints 1 and 6 of the fixed platform, axis *zf* perpendicular to the plane of the fixed platform pointing up and axis *yf* completing the right-hand rule. The other system has the origin in the center of the movable platform *M* and axis *xm* pointing between joints 1 and 6 of the movable platform, axis *zm* perpendicular to the plane of the movable platform pointing upward and axis *ym* completing the right-hand rule. Figure 2 shows the orientations of the two coordinate systems.

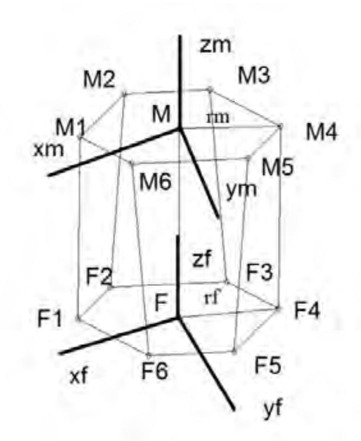

Figure 2: Coordinate systems for fixed and movable platforms

The positions of the joints of the fixed platform, F_i, and the movable platform, M_i, in the coordinate systems of the fixed and movable platforms respectively are expressed by Eqs. (1), (2), (3) and (4).

$$\{F_i\}^F = \{rf\cos(\Lambda f_i) \quad rf sin(\Lambda f_i) \quad 0\}^T = \{F_{i1} \quad F_{i2} \quad 0\}^T,\ i = 1,2,\dots,6 \tag{1}$$

$$\{M_i\}^M = \{rm\cos(\Lambda m_i) \quad rm sin(\Lambda m_i) \quad 0\}^T = \{M_{i1} \quad M_{i2} \quad 0\}^T \tag{2}$$

$$\Lambda f_i = 60°i - \lambda f,\ \Lambda m_i = 60°(i-1) + \lambda m, \quad i = 1,3,5 \tag{3}$$

$$\Lambda f_i = 60°(i-1) + \lambda f, \quad \Lambda m_i = 60°i - \lambda m, \quad i = 2,4,6 \tag{4}$$

where *rf* and *rm* are the radii of the circles centered at the center of the platforms and contain the positions of the joints of the fixed and movable platforms, respectively, and λf and λm are angles that help to define the positions of the joints of the fixed and movable platforms, respectively.

The set of joints positions, the vector representing the actuator in the fixed platform coordinate system $\{V_i\}^F$ is obtained using equation (5).

ISSN 2176-5480

$$\{V_i\}^F = \{M_i\}^F - \{F_i\}^F \tag{5}$$

The vector representing the position of the joints of the movable platform in the fixed coordinate system is defined in Eq. (6).

$$\{M_i\}^F = \{M\}^F + [T^{MF}] \times \{M_i\}^M = \begin{Bmatrix} x \\ y \\ z \end{Bmatrix} + \begin{Bmatrix} u_i \\ v_i \\ w_i \end{Bmatrix} \tag{6}$$

where $\{M\}^F$ is the vector that represents the position of the center of the movable platform in the coordinate system of the fixed platform and $[T^{MF}]$is the transformation matrix of the movable coordinate system to the fixed coordinate system.

Using a sequence of three rotations, it is possible to obtain the transformation matrix $[T^{MF}]$. First, a rotation φ around the axis *xm* is applied until axis *ym* becomes parallel to the plane formed by *xf* and *yf*, and the rotation angle φ is called roll angle. Then, a rotation θ around *ym* is applied until *xm* is parallel to the plane formed by *xf* and *yf*, being θ the pitch angle. Finally, a rotation ψ around *zm* is applied until *xm* is parallel to *xf*, and ψ is the yaw angle. The resulting matrix of the three rotations is presented in Eq. (7).

$$[T^{MF}] = \begin{bmatrix} c\varphi c\theta & c\varphi s\theta s\psi - s\varphi c\psi & c\varphi s\theta c\psi + s\varphi s\psi \\ s\varphi c\theta & s\varphi s\theta s\psi + c\varphi c\psi & s\varphi s\theta c\psi - c\varphi s\psi \\ -s\theta & c\theta s\psi & c\theta c\psi \end{bmatrix} \tag{7}$$

where *c* is the cosine of the angle and *s* is the sine.

The vector representing the *i* th-order actuator $\{V_i\}$ is obtained using information about the geometry of the Stewart platform and the set of positions and attitudes of the movable platform. The module of this vector $|V_i|$ is equal to the length of the actuator it represents.

2.1 **Actuator Model**

For the movable platform to remain in the desired position and attitude with respect to the fixed platform, it is necessary to control the length of the actuator. An electromechanical actuator was tested and modeled to represent all the actuators in this paper. This actuator consists of an electric motor with gear transmission for a ball screw. The motor is actuated by a voltage signal with amplitude of up to 12V, and changes its direction of rotation when the polarization is reversed. To feed this engine, we used a drive speed control for brushed motors RoboClaw 2; this drive receives a signal from 0V to 2V and converts it to a signal from -12V to 12V. An 1250 points encoder was installed around the shaft of the motor with the function of measuring the number of revolutions of the engine.

Two experiments were accomplished to the actuator model. For both system tests, the acquisition, processing and transmission *dSPACE®* system was used to send the signal 0V to 2V to the speed control driver and to receive the signal from the encoder.

The first test was used to obtain the actuator length variation in relation to the number of engine revolutions. In this test, the engine was fired to increase the length of the actuator until some positions along its course, and then the number of rotations of the motor and the actuator length were measured.

The relationship between the stroke length and the number of revolutions of the engine was obtained using the method of least squares to obtain the coefficients of the calibration line with the least squared error with respect to the points obtained in the experiment. Equation (8) shows the equation of the calibration line obtained in this process.

$$y_c = 0{,}000813P + 7{,}8485 \tag{8}$$

where *yc* is the stroke length in millimeters and *P* is the number of motor rotations in points of the encoder.

The characteristics of the dynamic response of the actuator were obtained in the second experiment. In this test step voltage inputs to the motor were applied and the lengths of strokes of the actuator were measured by reading the encoder in conjunction with Eq. (8). Figure 3 shows the variation of the strokes lengths of the engine when a -12V signal was applied to the engine.

It can be seen that the course reduces its length as the signal voltage is applied, stopping only within the limits of displacement.

ISSN 2176-5480

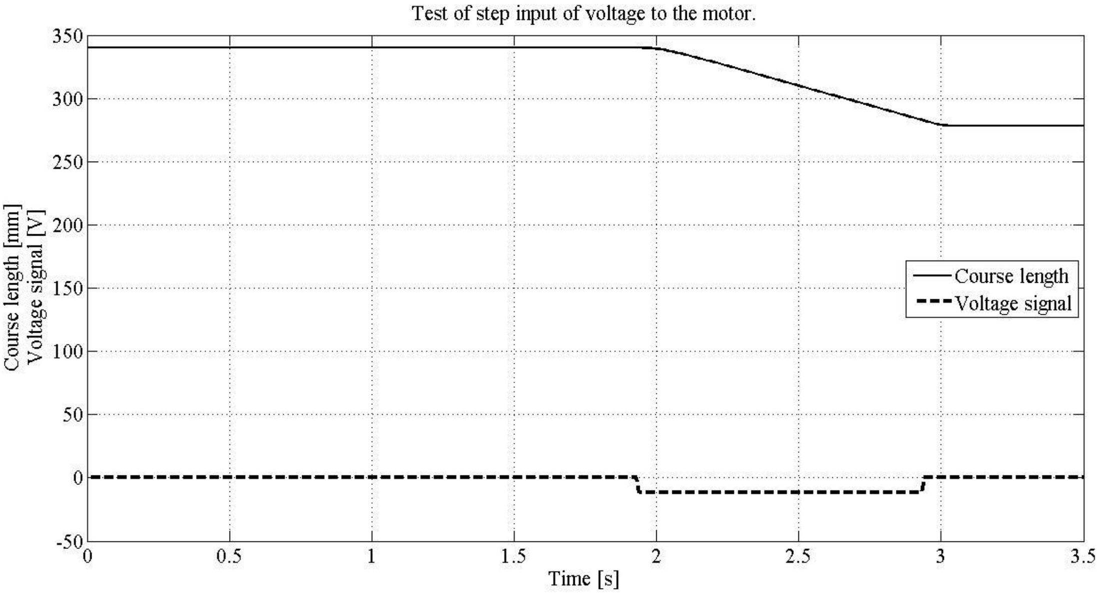

Figure 3: Test of step input of - 12V to the motor.

Limited information can be obtained using the actuator displacement response to a step input, but looking at the speed response of the actuator as shown in Fig. 4, one can see how it behaves when a step input of -12V is applied. The average speed of the system is approximately -62.66 mm/s in steady state regime.

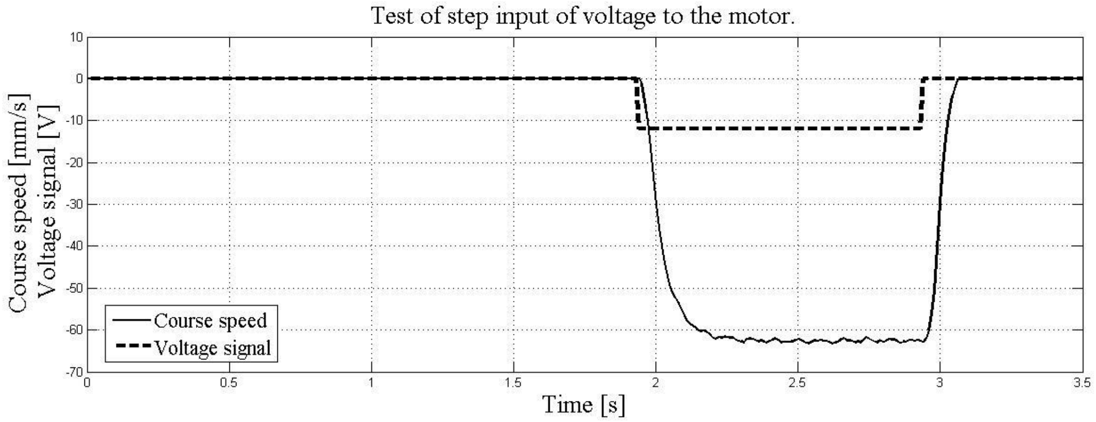

Figure 4: Actuator speed response to a step input of-12V.

Based on the response to -12V step input shown in Fig. 4, and responses to step inputs, 12V, 10V, 5V, -5V and -10V not shown here one could note that the system responds exponentially and in steady state has a characteristic oscillation increased noise. Then it was decided to use as a model for the transfer function of the actuator speed to voltage input signal, a third order system composed by summing a first order system and a second order system, as shown by Eq. (9).

$$\frac{Y(s)}{U(s)} = \frac{k_1\omega^2}{s^2+\omega^2} + \frac{k_2}{s+a} = \frac{k_2 s^2 + k_1\omega^2 s + \omega^2(k_2 + k_1 a)}{s^3 + as^2 + s\omega^2 + a\omega^2} \tag{9}$$

where k_1 and k_2 are the gains of the subsystems of first and second order, respectively,. ω is the natural frequency of the second order system and a is the pole of the first order system. Y(s) U(s) are the Laplace transforms of the actuator speed and the voltage signal, respectively.

The system characteristics of Eq (9) can be obtained by comparing the speed actuator response with the response characteristics of a third order system to a step input (D'Azzo; Houpis, 1995) e (Ogata, 1997).

Therefore, the natural frequency ω is equal to the oscillation frequency in steady state, the gain k_1 is the quotient of dividing the oscillation amplitude A_0 by the value of the step input u_D, as shown in Eq. (10), thus completing the characteristics of the second-order system.

ISSN 2176-5480

$$k_1 = \frac{A_0}{u_D} \tag{10}$$

The quotient dividing the gain k_2 to the pole is equal to the actuator average speed, y_M , in steady state, subtracted from the product of the gain k_1 with the value of step input u_D, as shown in Eq. (11); the pole can be obtained using a point before the system enters in regime in conjunction with Eq. (12) and to complete the characteristics of the first order system, gain k_2 can be found using Eq. (13).

$$\frac{k_2}{a} = y_M - k_1 u_D \tag{11}$$

$$a = \frac{\ln\left(\frac{a}{k_2}\left(k_1 + \frac{k_2}{a} + y(ti) - k_1 \cos\left(\omega(t_i - t_0)\right)\right)\right)}{t_i - t_0} \tag{12}$$

where t_i is the time at which the sample was obtained, t_0 is the time of occurrence of the step input and $y(t_i)$ is the speed at time t_i.

$$k_2 = \left(\frac{k_2}{a}\right) a \tag{13}$$

In this experiment, it was observed that the actuator has a dead zone between -1.365 V and 1.953 V. In this voltage range, the actuator does not change its length, but outside this range, the velocity of the system increases linearly. To overcome this characteristic, instead of using the value of the step input in Eqs. (10), (11), (12) and (13) one can use the value of the effective input step u_E defined in Eq. (14).

$$u_{DE} = \begin{Bmatrix} u_D - 1{,}9353, se \quad u_D > 1{,}9353 \\ 0, se \quad -1{,}365 \le u_D \le 1{,}9353 \\ u_D + 1{,}365, se \quad u_D < -1{,}365 \end{Bmatrix} \tag{14}$$

Because of the presence of noise in the speed response of the actuator, average values of the characteristics were used. As the length of the actuator is the integral of velocity, the transfer function of the length of the actuator to the effective voltage signal can be represented by Eq. (15).

$$\frac{Y_C(s)}{U_E(s)} = \frac{Y(s)}{U_E(s)} \times \frac{1}{s} = \frac{k_2 s^2 + k_1 \omega^2 s + \omega^2(k_2 + k_1 a)}{s^4 + a s^3 + \omega^2 s^2 + a\omega^2 s} \tag{15}$$

where $Y_C(s)$ and $U_E(s)$ are the Laplace transforms of the actuator length and the effective voltage signal, respectively. The Eq. (16) shows the transfer function of the actuator.

$$\frac{74{,}75 s^2 + 312 s + 4{,}819e005}{s^4 + 12{,}79 s^3 + 6394 s^2 + 8{,}177e004 s} \tag{16}$$

3. PID CONTROLLER

We used the PID controller which is widely known, with transfer function presented in equation 17. A controller was designed and this was applied to each of the six actuators independently (Moretti, 2010). The block diagram of the Stewart Platform control system is present in Fig.5. The controller takes as input the signal from the error between the desired actuator length and actual length and then defines the control action that is the sum of proportional, derivative and integrative actions.

$$\frac{U_E}{E}(s) = \frac{kd\left(s^2 + \frac{kp}{kd}s + \frac{ki}{kd}\right)}{s} \tag{17}$$

ISSN 2176-5480

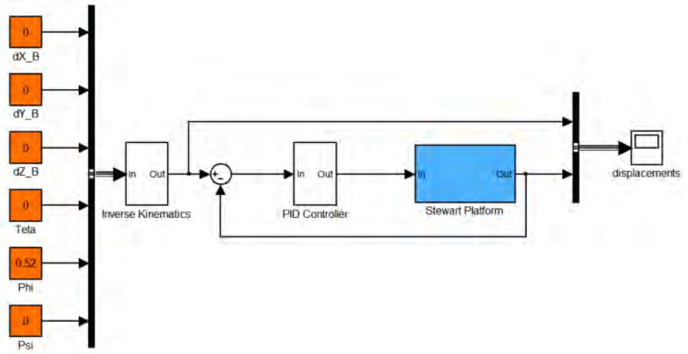

Figure 5: Block Diagram of the Stewart Platform Control System

4. RESULTS AND CONCLUSIONS

Tests and simulations were performed using zero initial conditions and varying displacements *dy* and *dz*.

Figure 6 illustrates the responses to 50 mm step input in *dz* experiment parameter. The steady state regime occurs after 7 seconds and has an overshoot 7 to 10 mm.

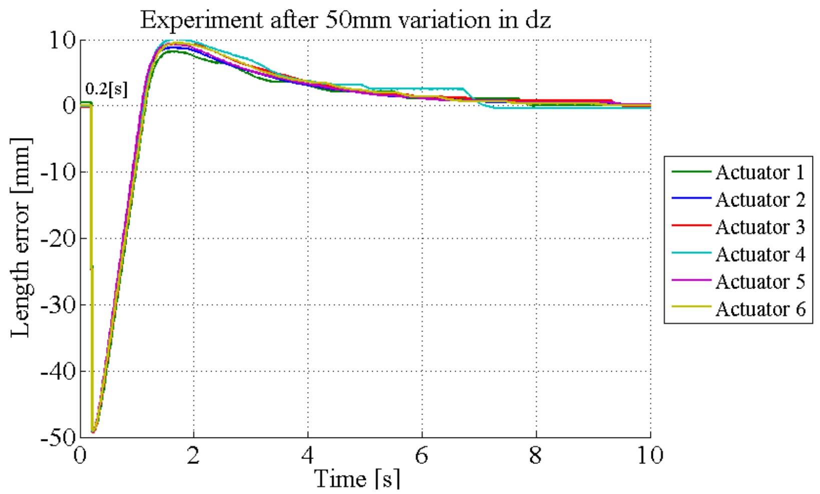

Figure 6: Experiment of 50mm variation in *dz*

The simulation of 50mm variation in *dz* parameter is illustrated in Fig. 7. The steady state regime is 6 seconds and has an overshoot of 5 mm.

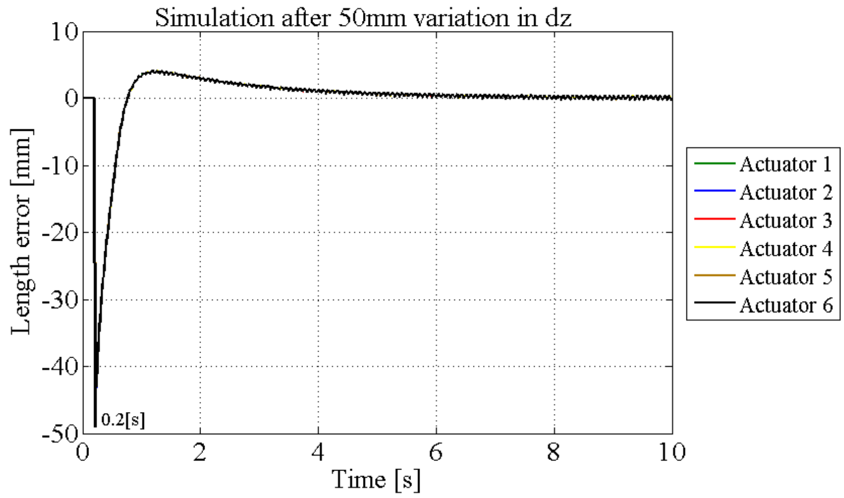

Figure 7: Simulation of 50mm variation in *dz*

Using as reference the first actuator, Fig. 8 compares the real actuator displacement with the simulated displacement. The simulation reaches the desired signal with a lower overshoot.

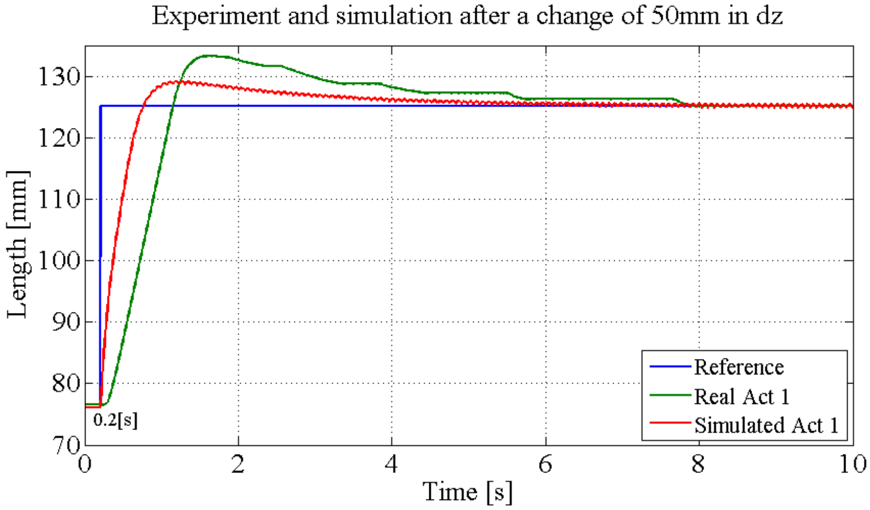

Figure 8: Experiment and simulation of a variation of 50mm in *dz*.

Another test is done with a step of 50mm applied to the term *dy*. Figure 9 shows the error of each actuator length of the experiment. The actuators reach the desired value in about 7 seconds.

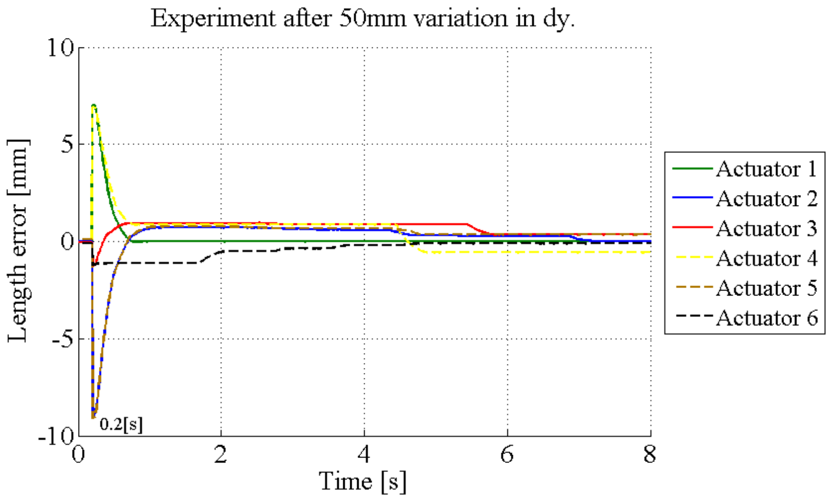

Figure 9: Experiment of 50mm variation in *dy*.

A step input of 50mm *dy* is applied in the simulation. Figure 10 illustrates the error of the length of each actuator. The simulation also reaches the desired value in about 7 seconds.

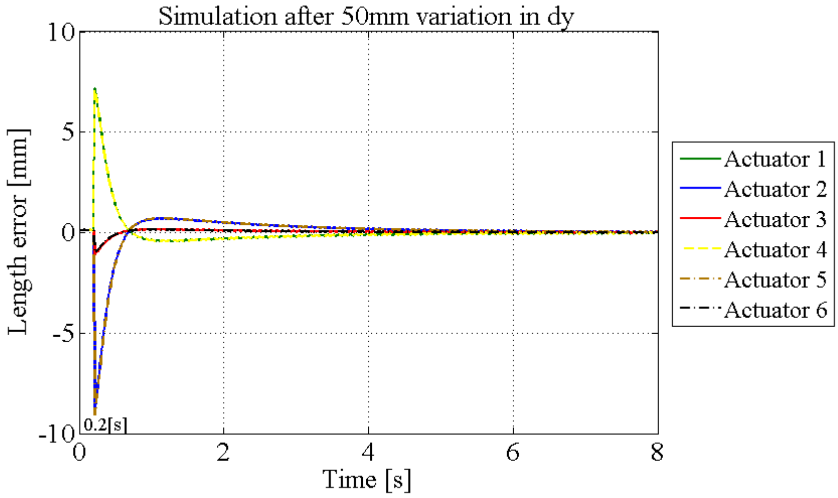

Figure 10: Simulation of 50mm variation in *dy*.

A comparison between experiment and simulation using actuator 1 as reference is shown in Fig. 11 where one can see that the desired value is achieved in 7 seconds, both in simulation and in the real experiment.

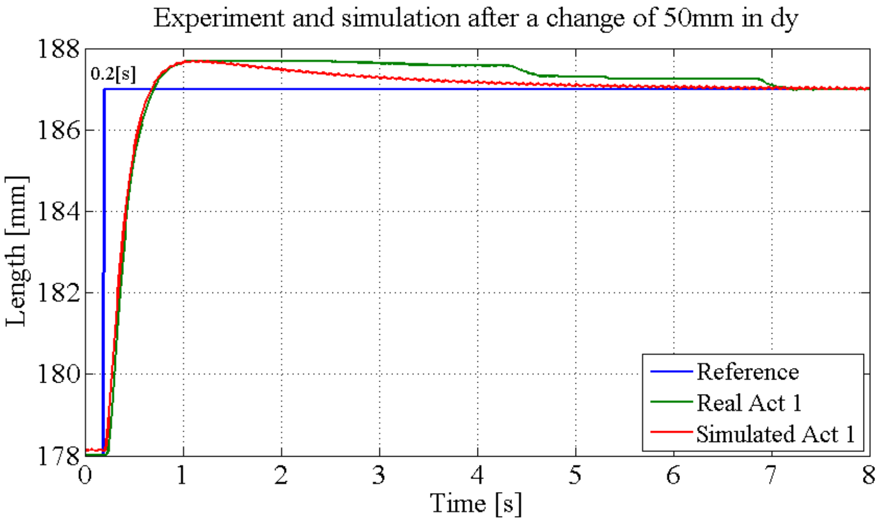

Figure 11: Experiment and simulation of a change of 50mm in *dy*.

The results show that the desired values are reached in about 7 seconds.

Figure 8 and Figure 11 show that the tests and simulations take the same time to reach the desired value. We can say that the PID controller used in this work was efficient and satisfactory for attitude and position control of the Stewart Platform, since the error tended to zero in all conditions tested.

5. ACKNOWLEDGEMENTS

The financial support of CNPq is gratefully acknowledged.

6. REFERENCES

BECERRA-VARGAS, M., 2009. “Control Platform Motion of a Flight Simulator ” 172 p. Thesis (Ph.D. in Mechanical Engineering), Escola de Engenharia de São Carlos, Universidade de São Paulo, São Carlos.

DASGUPTA, B.; MRUTHYUNJAYA, T.S., 2000. “The Stewart Platform Manipulator: a review”. Mechanism and Machine Theory 35. 15-40 p. Pergamon.

D’AZZO, J. J.; HOUPIS, H. C., 1995. “Linear control system analysis and desing: conventional and modern”. 3th ed., New York, McGraw Hill Publishing Company.

ISSN 2176-5480

MORETTI, Mariana, 2010. " Dynamic study and simulation of a Stewart platform with emphasis on the implementation of the control system" 121 p. Dissertation (Master in Mechanical Engineering), Universidade Estadual de Campinas, Faculdade de Engenharia Mecânica, Campinas.

NGUYEN, C. C. et al., 1993. "Adaptive control of a Stewart Platform-Based manipulator". Journal of Robotic Systems, v.10, n.5, p.657-87.

ZIPFEL, P. H., 2000. "Modeling and simulation of aerospace vehicle dynamics". Reston, VA: American Institute of Aeronautics and Astronautics. 551p.

OGATA, K., 1990, "Modern Control Engineering". 3. ed. New Jersey: Prentice Hall, 961p.

STEWART, D., 1965. "A platform with six degrees of freedom". Proceedings of Institution of Mechanical Engineers, Part 1, v.180, n.15, p.371-86.

7. RESPONSIBILITY NOTICE

The authors are the only responsible for the printed material included in this paper.